https://doi.org/10.1016/j.bmc.2019.02.024

This is the Pre-Published Version.

Antibacterial activity of indolyl-quinolinium derivatives and study their mode of action

Senyuan Cai[a,#], Wenchang Yuan[b, #], Ying Li[a], Xuanhe Huang[a], Qi Guo[c], Ziwei Tang[d], Zhiyuan Fang[b], Hai Lin[b], Wing-Leung Wong[e], Kwok-Yin Wong[e,*], Yu-Jing Lu[a,*], Ning Sun[a,b,e,*]

[a.] School of Chemical Engineering and Light Industry, School of Biomedical and Pharmaceutical Sciences, Guangdong University of Technology, Guangzhou 510006, P.R. China; E-mail: luyj@gdut.edu.cn;

[b.] The Fifth Affiliated Hospital of Guangzhou Medical University, Guangzhou 510700, P.R. China; E-mail: ning.sun@connect.polyu.hk;

[c.] State Key Laboratory of Ophthalmology, Zhongshan Ophthalmic Center, Sun Yat-sen University, Guangzhou, P.R. China;

[d.] School of Pharmaceutical Sciences, Guangzhou Medical University, Guangzhou, P.R. China;

[e.] The State Key Laboratory of Chemical Biology and Drug Discovery, Department of Applied Biology and Chemical Technology, The Hong Kong Polytechnic University, Hung Hom, Kowloon, Hong Kong, China.

# These authors contributed equally to this paper.

* Corresponding authors

© 2019. This manuscript version is made available under the CC-BY-NC-ND 4.0 license https://creativecommons.org/licenses/by-nc-nd/4.0/.

Abstract

Filamenting temperature-sensitive mutant Z (FtsZ) is recognized as a promising target for new antibiotics development because of its high conservatism and pivotal role in the bacteria cell division. The aromatic heterocyclic scaffold of indole is known showing merit medical functions in antiviral and antimicrobial. In the present study, a series of 1-methylquinolinium derivatives, which were integrated with an indole fragment at its 2-position and a variety of amino groups (cyclic or linear, mono- or di-amine) at the 4-position were synthesized and their antibacterial activities were evaluated. The results of antibacterial study show that the representative compounds can effectively inhibit the growth of testing strains including MRSA and VRE, with MIC values of 1 to 4 μg/mL by bactericidal mode. The mode of action assays revealed that **c2** can effectively disrupt the rate of GTP hydrolysis and dynamic polymerization of FtsZ, and thus inhibits bacterial cell division and then causes bacterial cell death. In addition, the result of resistance generation experiment reveals that **c2** is not likely to induce resistance in *S. aureus*.

Keywords: Indolyl quinolinium derivatives, antibacterial activity, drug resistant bacteria, FtsZ, cells division.

1. Introduction

The emergence of multidrug resistance among clinically significant bacterial pathogens is now being a worldwide public health issue. The high morbidity and mortality rates could be expected in the future due to lack of effective drugs to treat with the infections from these super bacteria.[1] However, new drugs development against the multidrug resistant infection is a big challenge. Currently, the first-line clinical antibiotics display weak or even no activity against resistant bacteria,[2] the

development of new types of antibacterial agents that possess a novel mechanism of action is therefore an urgent need.[3]

Target selection in new medicines research is critical. Bacterial divisions are currently believed to be a new area for new generation of antibiotics development because it has a complex set of biochemical machinery containing many functional proteins that control cell division process.[4] Among these proteins, filamenting temperature-sensitive mutant Z (FtsZ) is highly conserved among bacterial pathogens but not found in the mammalian cells.[5] Therefore, it could be the right target for drug discovery. As a matter of fact, FtsZ plays a very essential role in the process of bacterial cell division. In the beginning of bacterial cell division, FtsZ, a GTPase, assembles into protofilaments and forms the ring-like structure (called the Z-ring) in a GTP-dependent manner at middle of the cell.[6] This ring makes a great contribution to the cell membrane and serves as a scaffold for the recruitment of many functional proteins, completing the bacterial cell division.[6,7] It is obvious that any factor disrupting the dynamic assembly or/and GTP hydrolysis of FtsZ could eventually cause the failure of bacterial cell division and then bacterial cell death. As FtsZ taking such an essential role in cell division and being an unexploited drug target, it has become a majority interest in the exploration in recent years.[8]

Over the past decade, efforts have been continuously devoted to the development of FtsZ inhibitors and many of them are exhibiting potency of disrupting FtsZ function.[5,8,9] Zantrins (Fig. 1A) and N-methylbenzofuro quinoline derivative were used to study FtsZ polymerization dynamics and proliferation inhibition effects of bacterial strains.[10,11] A quinoline derivative (Fig. 1B) was also found to inhibit the mycobacterial FtsZ by disrupting the polymerization of *Mtb*FtsZ.[12] Recently, a quinolinium derivative (Fig. 1C) was reported for its superior antibacterial activity and disruption of GTPase activity.[13] As the molecular scaffold of this quinolinium derivative has been demonstrated as a very useful pharmacophore, the further introduction of a suitable hydrophobic side chain or an aromatic heterocyclic moiety into its framework could be helpful in enhancing their interactions with the

hydrophobic pocket of FtsZ.[14] On the other hand, nitrogen-containing compounds have been widely adopted in molecular design for new drug discovery.[15] We speculate that this rational design may result in a significant improvement in the on-target activity and the antibacterial activity. In the present study, a series of compounds (Fig. 1D: **c1-c15**) developed from the molecular fusion of quinolinium-indole-amine was studied for the first time to explore their antimicrobial activities and the mode of action targeting FtsZ protein.

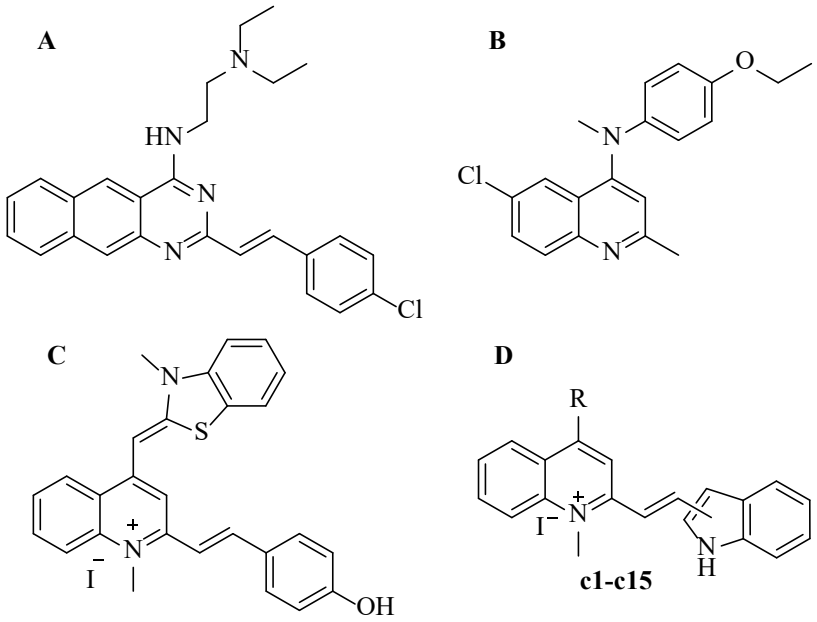

Fig. 1. Structures of zantrin Z3 (A), quinoline derivative (B), quinolinium derivative (C), and indolyl quinolinium derivatives (D).

2. Results and discussion

2.1. Synthesis of quinolinium-indole-amine fused derivatives

The target compounds **c1 – c15** were prepared in good yields by the integration of 1-methylquinolinium and an indolyl-vinyl fragment through a straightforward two-step synthesis process[16] (Scheme 1). The intermediates (1-methylquinolinium iodide or chloro-methylquinolinium iodide) were obtained by the methylation reaction of 2-methylquinoline, and 4-chloro-2-methylquinoline with iodomethane in the presence of sulfolane. Further condensation reaction of the intermediate with suitable

indolyl carbaldehyde and different amides in one-pot can attain the target compounds. All the compounds reported herein were characterized by ^{1}H NMR, ^{13}C NMR and HRMS. Among these compounds, **c1**, **c5** and **c7 – c8** were reported as bio-molecular sensing probe by our group.[16-18]

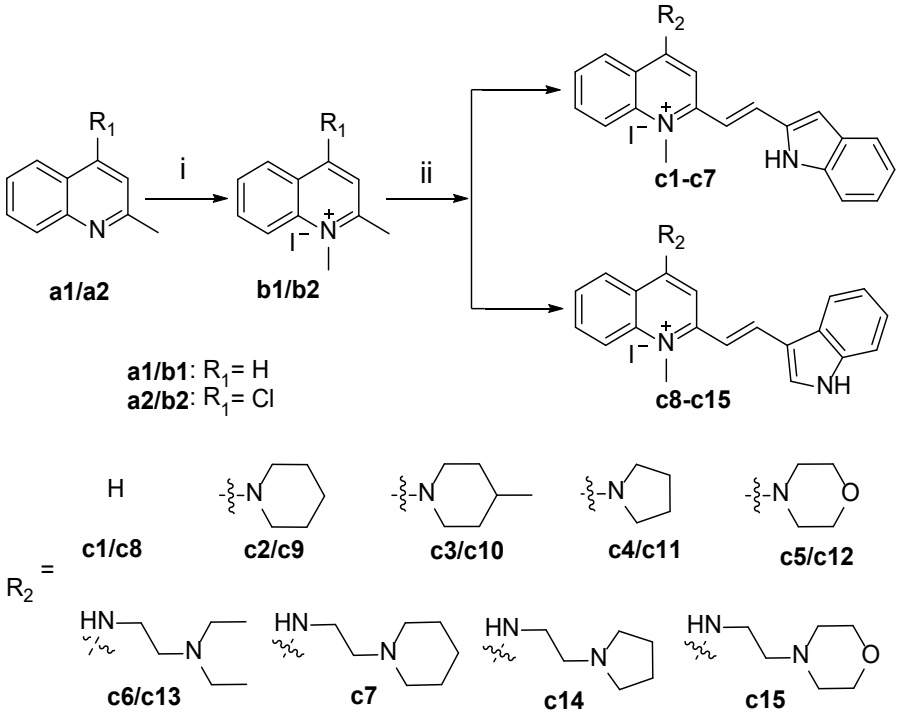

Scheme 1. Synthetic routes of indolyl quinolinium derivatives (**c1**–**c15**). Reagents and conditions: (i) iodomethane, sulfolane, 60 °C for 8 h; (ii) 1H-indole-2-carbaldehyde/1H-indole-3-carbaldehyde, amines, anhydrous ethanol 70 °C for 6 h.

2.2. Antibacterial susceptibility assays

The minimum inhibitory concentrations (MICs) of the quinolinium derivatives were tested against Gram-positive (Table 1) and Gram-negative (Table 2) bacteria by broth microdilution procedures described in the Clinical and Laboratory Standards Institute (CLSI) guidelines.[19] The determined MICs values were compared with penicillin, ciprofloxacin, and vancomycin under the same assay conditions for antimicrobial susceptibility assessment. The results showed that the inhibition effect of these compounds on gram-positive bacteria was generally better than that of gram-negative bacteria, indicating that these compounds had good potential to

develop further into effective antibacterial agents against gram-positive bacteria. In addition, for certain potent compounds, they can inhibit the growth of the tested gram-positive strains, including drug-resistant strains, with MIC values lower than 10 μg/mL (Table 1). It is interesting to observe that these most active compounds (**c2**, **c9**) possess a common piperidine group at the 4-position of the 1-methylquinolinium core, indicating that the integration of these substituent is the key contribution to excellent potency of antibacterial activity. The results show that the compounds containing amino substituents including piperidine (**c2**/**c9**), 4-methylpiperidine (**c3**/**c10**), pyrrolidine (**c4**/**c11**) at the 4-position of the 1-methylquinolinium core, have a better antibacterial activity than that have 2-diethylaminoethylamine (**c6**/**c13**), 2-piperidinoethylamine (**c7**), 2-pyrrolidinoethylamine (**c14**), 2-morpholinoethylamine (**c15**). Among all these compounds, **c2** and **c9** are showing the best inhibition ability against *S. aureus* ATCC 29213 with the MIC values of 1 μg/mL, which are comparable or even superior to the three antibiotic references. From Table 2, some of the compounds also showed moderate to good inhibitory activity against Gram-negative bacteria. It seems that compounds **c2**/**c9** and **c3**/**c10** possess higher potency against *E. coli* ATCC 25922 and ATCC BAA-2469 than other derivatives probably due to the common-shared piperidine or 4-methylpiperidine substituent group at the 4-position of the 1-methylquinolinium core. Interestingly, this observation in inhibition activity is similar to that found in the treatment with Gram-positive bacteria shown in Table 1. Therefore, the inclusion of piperidine and indole scaffolds could be somehow important for the consideration in new molecular drug design against Gram-positive bacteria targeting at the inhibition of FtsZ protein activity.

Table 1 Minimum inhibitory concentrations (MICs) of compounds against Gram-positive bacteria strains (μg/mL).

Bacterial strains

	B. subtilis 168	*S. aureus* ATCC 25923	*S. aureus* ATCC 29213[b]	*S. aureus* ATCC BAA-41[c]	*S. aureus* ATCC 43300[c]	*E. faecium* ATCC 700221[d]	*E. faecium* ATCC 49624	*E. faecalis* ATCC 29212
Pen[a]	32	<0.125	>64	>64	>64	>64	0.25	0.5
Cip[a]	2	<0.125	2	>64	2	>64	32	4
Van[a]	0.25	2	2	2	2	>64	0.5	2
c1	32	32	32	32	64	64	32	32
c2	4	1	1	2	2	4	2	4
c3	8	4	4	8	8	8	4	8
c4	8	4	2	8	8	16	8	16
c5	8	16	16	16	16	32	16	64
c6	16	16	16	32	64	64	32	64
c7	16	16	16	32	32	32	16	64
c8	32	32	32	32	32	64	32	32
c9	4	2	1	2	4	4	2	4
c10	4	2	4	4	4	4	2	4
c11	8	4	2	4	16	8	4	16
c12	16	16	16	32	32	32	16	16
c13	16	16	16	32	32	64	32	64
c14	32	16	16	64	64	64	32	64
c15	64	64	32	64	64	64	32	64

[a.] Pen: penicillin; Cip: ciprofloxacin; Van: vancomycin; [b] penicillin-resistant strain; [c] methicillin-resistant strain; [d] vancomycin-resistant strain; Other strains are drug susceptible strains.

Table 2 Minimum inhibitory concentrations (MICs) of compounds against Gram-negative bacteria strains (μg/mL).

	Bacterial strains					
	E. coli ATCC	*E. coli* ATCC	*A. baumannii* ATCC	*K. pneumonia*e ATCC	*P. aeruginosa* ATCC	*E. cloacae* ATCC

	25922	BAA-2469[b]	19606[c]	BAA-2470[b]	BAA-2108[c]	BAA-1143[d]
Pen[a]	1	>64	64	>64	>64	>64
Cip[a]	<0.125	>64	2	64	64	0.5
Van[a]	>64	>64	64	>64	>64	>64
c1	64	64	>64	>64	>64	>64
c2	16	16	32	>64	>64	>64
c3	32	32	>64	>64	>64	>64
c4	32	32	64	>64	>64	>64
c5	64	64	>64	>64	>64	>64
c6	64	64	>64	>64	>64	>64
c7	32	64	64	>64	>64	>64
c8	>64	>64	>64	>64	>64	>64
c9	8	16	16	>64	>64	>64
c10	16	32	32	>64	>64	>64
c11	32	32	64	>64	>64	>64
c12	64	>64	>64	>64	>64	>64
c13	64	64	>64	>64	>64	>64
c14	64	64	>64	>64	>64	>64
c15	>64	>64	>64	>64	>64	>64

146 [a.] Pen: penicillin; Cip: ciprofloxacin; Van: vancomycin; [b] expressing NDM-1 beta-lactamase; [c]
147 multidrug-resistant strain; [d] expressing AmpC beta-lactamase; Other strains are drug susceptible
148 strains.

149

150 *2.3. Bactericidal or bacteriostatic assay*

151 Based on the MICs results, we further assessed the minimum bactericidal
152 concentrations (MBCs) of the selected compounds against methicillin susceptible *S.*
153 *aureus* ATCC 29213 and MRSA ATCC BAA-41. Vancomycin was used as a control
154 for the tests. According to the CLSI standards, an MBC/MIC ratio of 1-2 is considered
155 as indicative of bactericidal behavior. By contrast, for the MBC/MIC ratio $\geqq$ 8 is

considered indicative of bacteriostatic behavior.[20] The results listed in Table 3 showed that vancomycin was observed as bactericidal agents with the MBC/MIC ratios of 1 against two *S. aureus* strains (The results of time-killing kinetics assay can be referred to ESI Fig. S47). For our compounds, **c2** and **c9** also exhibited a bactericidal mode against both methicillin susceptible and resistant *S. aureus* with the MBC/MIC ratio of 2.

Table 3 Comparison of MIC and MBC Values for **c2** and **c9** against two *S. aureus* strains.

Comp	MBC(μg/mL)	MIC(μg/mL)	MBC/MIC
	S. aureus ATCC 29213		
c2	2	1	2
c9	2	1	2
vancomycin	2	2	1
	S. aureus ATCC BAA-41		
c2	4	2	2
c9	4	2	2
vancomycin	2	2	1

2.4. Time-killing kinetics determinations

In order to further study the antibacterial activity of compounds, time-kill kinetics assays monitored by the viable counts method were used to confirm the bactericidal property of **c2** against *S. aureus* ATCC BAA41. As shown in Fig. 2A, the bacterial cells grew rapidly in the first 8 h without **c2**. After 8 h incubation, the growth of *S. aureus* went into the stationary phase. On the other hand, 2 × MIC and 4 × MIC of **c2** can rapidly reduce the viable counts (10^3 CFU mL^{-1}) of *S. aureus* after incubation for 4 h. The growth inhibition of different concentration gradient revealed that the rate at which **c2** killed *S. aureus* was dependent on the compound concentration. The higher the concentration of the compound applied, the greater the rates of killing resulted. Moreover, **c2** at the 1 ×, 2 ×, 4 × MIC concentrations caused a

similar reduction of nearly 1 × 10^3 CFU mL^{-1} for *S. aureus* in 24 h. The results indicated that **c2** inhibited the growth of *S. aureus* in a bactericidal manner.

2.5. Drug resistance study

To further evaluate the drug resistance of these compounds, we selected two commercial antibiotics (Rifampin and Norfloxacin) as the positive control against *S. aureus* ATCC29213. As shown in Fig. 2B, comparing with the positive control, the MIC values for **c2** and **c9** increased only 4-fold, while for rifampin and norfloxacin increased over 2000 and 500-fold of MIC values after 15 passages. The results showed that **c2** and **c9** exhibit potent antibacterial activity and may delay the development of drug resistance.

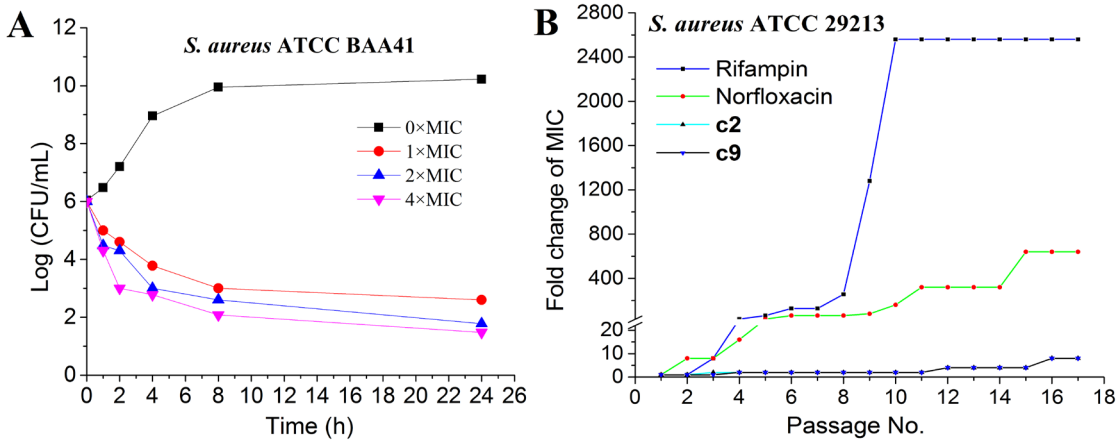

Fig. 2. (A) Time-killing Kinetics determinations for **c2**. At time zero, samples of a growing culture of *S. aureus* ATCC BAA41 were incubated with concentrations of **c2** equivalent to 1× (red), 2× (blue), or 4× (pink) the MIC. Vehicle (1% DMSO, black) was included. Samples were removed at the time intervals indicated for the determination of viable cell counts. (B) Bacterial resistance studies of rifampin, norfloxacin, **c2** and **c9** against *S. aureus* ATCC 29213.

2.6. Morphology and membrane integrity of B. subtilis cells

One characteristic of bacterial cell division inhibition observation is the cell elongation of an enlarged phenotype, which caused by disrupting the cell division function of FtsZ protein. Apart from this, the perturbation of membrane integrity may

cause bacterial cell lysis and death.[21] For these purpose, we investigated the bacterial cell morphology and membrane integrity by using a red fluorescent dye FM4-64 in the absence and in the presence of MIC concentration of the screened compounds from the antimicrobial susceptibility assessment. The observations were recorded by using a super high-resolution laser confocal microscopy. As shown in Fig. 3, **c2** remarkably increased the cell length of *B. subtilis* 168 from the range of 5-13 μm to 70-130 μm. Other compounds, **c9** and **c10** exhibited moderate effect on *B. subtilis* 168 (Fig. S1). Moreover, **c2** did not show any detectable impairment of cell membrane integrity (Fig. 4B) compared with the untreated bacterial cells (Fig. 4A). The results strongly indicated that **c2** inhibits the bacterial proliferation by disrupting the cell division function of FtsZ protein without perturbing the membrane integrity.

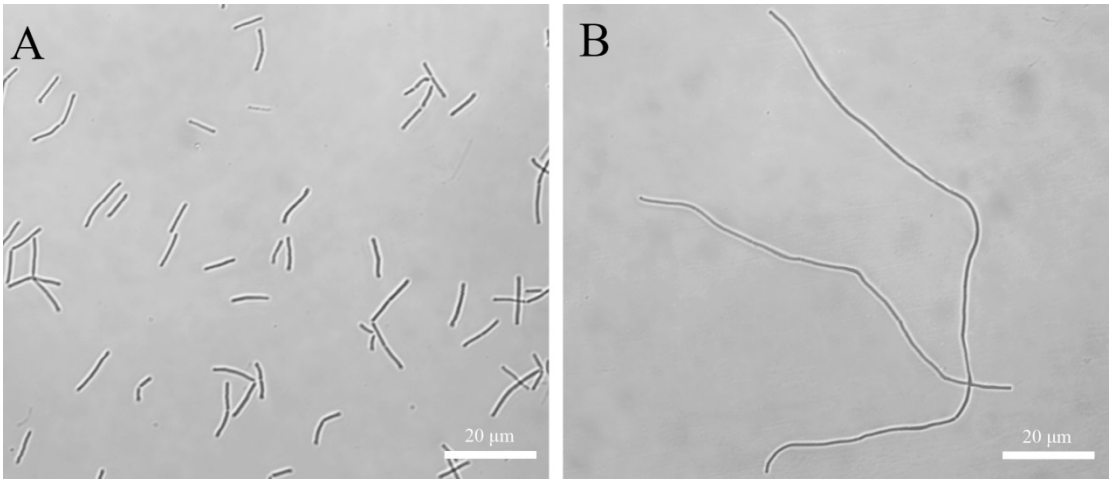

Fig. 3. The morphology of *B. subtilis*. Cells of *B. subtilis* 168 were grown in the absence (A) and presence of MIC concentration of **c2** (B). Scale bar = 20 μm.

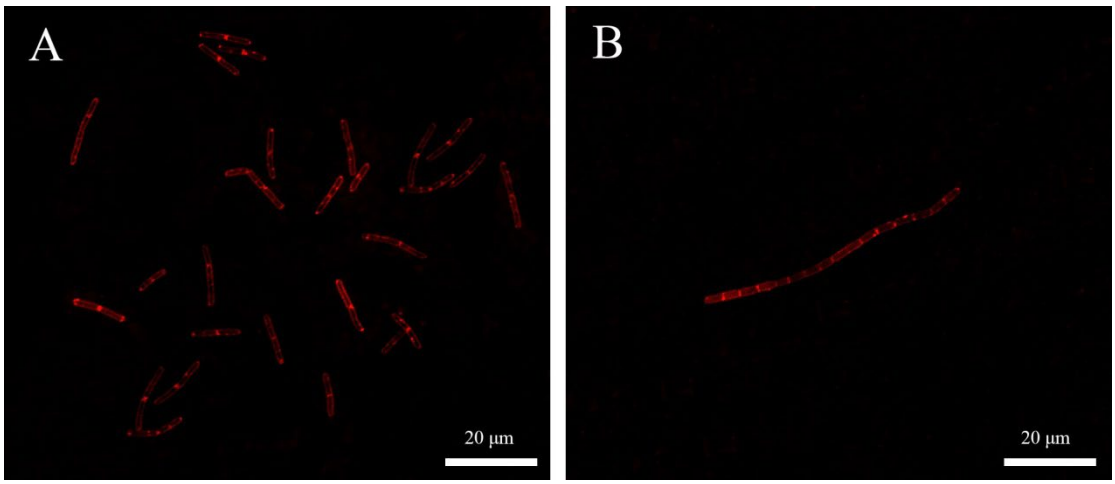

Fig. 4. The membrane integrity of *B. subtilis*. Cells of *B. subtilis* 168 were stained by red fluorescent dye FM4-64 in the absence (A) and presence of MIC concentration of **c2** (B). Scale bar = 20 μm.

2.7. Effects of indolyl quinolinium derivatives on the GTPase activity of FtsZ

A recent report showed that the dynamic polymerization of cell division protein FtsZ is dependent on the rate of GTP hydrolysis.[22] The possible mechanism of antibacterial activity inhibition was studied with two selected compounds (**c2** and **c9**), which possess better antibacterial activity. The effects of indolyl quinolinium derivatives on the GTPase activity were carried out. The interferential effects on the GTPase activity of FtsZ were shown in Fig. 5A and Table S1. The results show that both **c2** and **c9** inhibited GTP hydrolysis of FtsZ in a concentration-dependent manner. The GTPase activity of negative control (no compounds) is 19.8 units/L (ESI Table S1). The GTPase inhibitory effect of **c2** was found approximately 50% at the concentration of 32 μg/mL.

2.8. Light scattering assay

In the attempt to further investigate the mechanism of antibacterial activities with indolyl quinolinium derivatives, we used a light scattering assay to assess the effect of **c2** on the dynamic polymerization of FtsZ. Fig. 5B shows a time-dependent manner polymerization profiles of FtsZ in the absence and in the presence of **c2** at the

concentration ranged from 0.4 to 1.2 μg/mL. From the results, the compound exhibited an obvious enhancement effect on FtsZ polymerization at the concentration of 0.4 μg/mL compared with a negative control using DMSO conducted under the same conditions in the assay. The results indicate that the compound shows strong efficacy in the disruption of the *Sa*FtsZ polymerization with a dose-dependent manner.

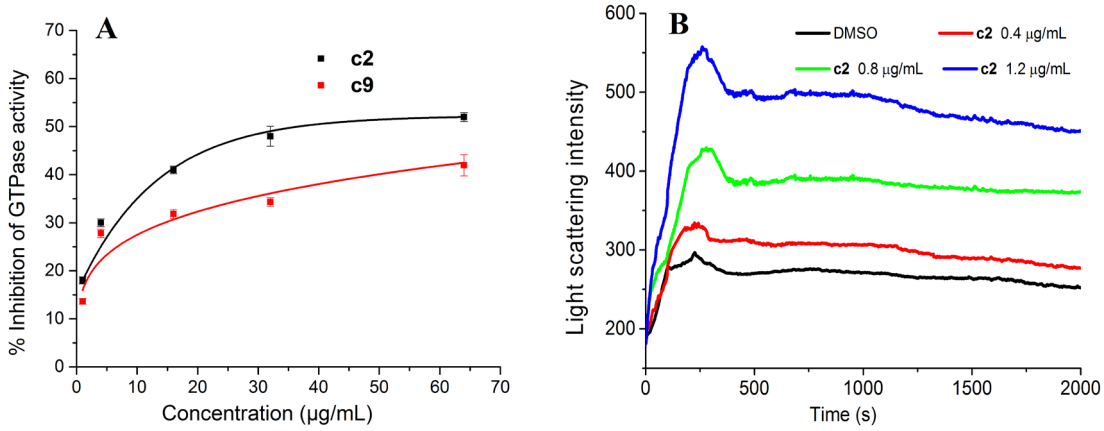

Fig. 5. (A) Inhibition of GTPase activity of FtsZ by compounds **c2** and **c9**. (B) Effect of indolyl quinolinium derivative (**c2**) on the polymerization of FtsZ.

*2.9. Antibacterial activity of **c2** and **c9** FtsZ over-expression strain*

To further confirm the *in vivo* on-target effect of the indolyl quinolinium derivatives, **c2** and **c9** were selected to test their antibacterial activity against a FtsZ over-expression strain (*E. coli* BL21). The over expression of FtsZ can be induced by IPTG. The MIC values of **c2** and **c9** were 8 μg/mL against this strain under non-over-expression condition. It is interesting to note that the MIC values of **c2** and **c9** increased to 32 and 16 μg/mL respectively, when FtsZ was over expressed (Table 4). The decline of antibacterial activity suggests that the over-expression FtsZ calls for more compounds to inhibit the function of FtsZ. The results suggest that **c2** and **c9** may interact with FtsZ *in vivo*.

Table 4 MIC of **c2** and **c9** against *E. coli* BL21 strain (μg/mL).

Compounds	*E. coli* BL21	*E. coli* BL21+IPTG
c2	8	32
c9	8	16

*2.10. Predicted binding mode of **c2** in FtsZ*

From the above biological assays, **c2** is ascertained as a potent FtsZ-targeting inhibitor. Molecular modeling study was used to further identify the potential binding site of the FtsZ protein with the compound. The optimal docking pose suggest that **c2** probably binds to a hydrophobic and narrow cleft constituted by the H7-helix, T7-loop and a four-stranded β-sheet (Fig. 6A). A 2D ligand interaction diagram (Fig. 6B) shows the predicted interactions between **c2** and FtsZ residues. The dominant binding of **c2** with Gln192, Gly196, Leu200, Val203, Leu209, Met226, Gly227, Ile 228, and Val297 of FtsZ protein are through hydrophobic interactions. In addition, an electrostatic interaction can be found between the positively charged amine and Asp199. Two carbon hydrogen bonds were found between the piperidine group of **c2** and Leu200/Val203. Moreover, a lot of amino acids in this pocket (such as Gly205, Val310, Ile311, etc.) can form van der waals force with **c2**.

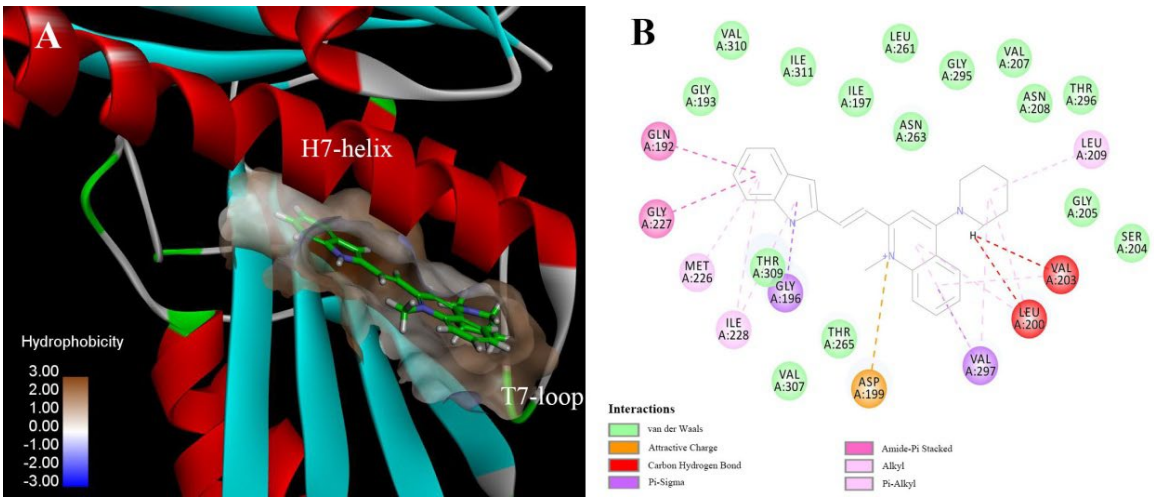

Fig. 6. (A) 1,2,4-trimethylquinolin-1-ium iodide derivatives (**c2**) was predicted to bind into the C-terminal interdomain cleft of FtsZ; (B) predicted interactions between **c2** and the amino acids of FtsZ.

3. Conclusions

In conclusion, we demonstrated a series of molecules fused with quinolinium-indole-amine in the FtsZ-targeted antibacterial applications for the first time. The class of compounds exhibit significant antibacterial activity against several clinically representative strains including some drug resistant bacterial strains. Some of the compounds displayed superior or comparable antibacterial activity to penicillin, ciprofloxacin, and vancomycin. Two compounds (**c2** and **c9**) were identified with strong antibacterial activity against MRSA with MIC values from 1 to 4 μg/ml respectively. Based on the morphology of *B. subtilis* cell, **c2** can remarkably increase the cell length of *B. subtilis* 168 by inhibiting bacterial cell division without perturbing the membrane integrity. The results of biochemical assays revealed that **c2** can effectively disrupt the GTPase activity and polymerization of FtsZ in a dose-dependent manner and it does not trigger the development of bacterial resistance. Based on these studies, these indolyl-quinolinium derivatives may be worth for further structural modification and conducting in-depth antibacterial research.

4. Materials and methods

4.1. Chemistry

All reagents and chemicals were purchased from commercial unless otherwise specified. All the solvents were of analytical reagent grade and used without further purification. Melting point measurement was carried out using a SRS Opti Mel automated melting point instrument without correction. High resolution mass spectra (HRMS) were recorded with Shi-madzu LCMS-IT-TOF. ^{1}H and ^{13}C NMR spectra were recorded in DMSO using TMS as the reference with a Bruker Bio Spin Gmb Hspectrometer at 400 MHz and 100 MHz, respectively. Reactions progress was monitored by thin-layer chromatography (TLC) on 0.25-mm pre-coated silica GF254 plates.

*4.2. General synthetic procedure for the intermediates **b1-b2***

Intermediates **b1**–**b2** were prepared according to similar previously reported protocol.[23] To the solution of 2-methylquinoline and 4-chloro-2-methylquinoline (0.2 g) in sulfolane (10 mL) were added iodomethane (0.42 mL, 6.74 mmol). The reaction mixture was stirred at 50 °C for 18 h, cooled and anhydrous ether is added after the shock, suction filtration, the solid was washed with anhydrous diethyl ether, and dried in vacuum to give of intermediates **b1**-**b2** in >80% yield.

*4.3. General synthetic procedure for indolyl quinolinium derivatives (**c1 - c15**).*

A solution of intermediates **b** (0.5 mmol), 1H-indole-2-carbaldehyde or 1H-indole-3-carbaldehyde, amides (3.6 mmol) in a closed pressure reactor with 10 mL anhydrous ethanol were heated to 70 ºC for reaction for 6 h. When the reaction mixture was cooled to room temperature, the mixture was poured into a beaker with 50 mL ether. Then the solution was filtered to remove solid and the filtrate was extracted with ether for three times (3 × 10 mL). The ether layers were combined and then were removed under reduced pressure. The obtained solid which is target compounds was dried in vacuum.

*4.3.1. (E)-2-(2-(1H-indol-2-yl)vinyl)-1-methylquinolin-1-ium iodide (**c1**)*

Purple solid, yield 76%; Melting point: 256–258 °C; ^{1}H NMR (400 MHz, DMSO-d_6) δ 11.94 (s, 1H), 9.29 (d, J = 6.5 Hz, 1H), 8.90 (d, J = 8.4 Hz, 1H), 8.49 (d, J = 6.5 Hz, 1H), 8.45 (d, J = 8.9 Hz, 1H), 8.35 – 8.22 (m, 3H), 8.12 (t, J = 7.7 Hz, 1H), 7.66 (d, J = 7.9 Hz, 1H), 7.50 (d, J = 8.2 Hz, 1H), 7.29 (t, J = 7.6 Hz, 1H), 7.08 (dd, J = 14.8, 7.1 Hz, 2H), 4.52 (s, 3H). ^{13}C NMR (100 MHz, DMSO) δ 154.0 (s), 147.0 (s), 139.2 (s), 139.0 (s), 138.0 – 138.1 (m), 135.0 (s), 133.5 (s), 129.0 (s), 126.6 (s), 125.9 (s), 125.8 (s), 123.6 (s), 122.0 (s), 120.8 (s), 119.4 (s), 115.1 (s), 113.8 (s), 113.2 (s), 113.1 (s), 44.4 (s). HRMS m/z: calcd. for $C_{20}H_{17}N_2$ $[M - I]^+$ 285.1386, found 285.1378.

*4.3.2. (E)-2-(2-(1H-indol-2-yl)vinyl)-1-methyl-4-(piperidin-1-yl)quinolin-1-ium iodide (**c2**)*

Brown solid, yield 50%; Melting point: 178 - 186°C; ^{1}H NMR (400 MHz, DMSO) δ 11.82 (s, 1H), 8.27 (d, J = 8.8 Hz, 1H), 8.11 (d, J = 8.3 Hz, 1H), 8.06 – 7.98 (m, 2H), 7.74 (t, J = 7.59 Hz, 1H), 7.63 (dd, J = 11.8, 9.1 Hz, 2H), 7.49 – 7.35 (m, 2H), 7.25 (t, J = 7.6 Hz, 1H), 7.06 (t, J = 7.5 Hz, 1H), 7.01 (s, 1H), 4.23 (s, 3H), 3.76 (s, 4H), 1.84 (s, 4H), 1.78 (s, 2H). ^{13}C NMR (100 MHz, DMSO) δ 160.0 (s), 153.6 (s), 141.4 (s), 138.9 (s), 136.0 (s), 134.1 (s), 133.5 (s), 128.4 (s), 127.0 (s), 126.4 (s), 124.9 (s), 121.8 (s), 120.5 (s), 120.2 (s), 119.6 (s), 117.6 (s), 112.0 (s), 109.8 (s), 104.4 (s), 56.5 (s), 53.3 (s), 40.6 (s), 40.4 (s), 40.2 (s), 40.0 (s), 39.8 (s), 39.6 (s), 39.4 (s), 38.4 (s), 25.9 (s), 24.0 (s), 19.0 (s). HRMS m/z: calcd. for $C_{25}H_{26}N_3$ $[M - I]^+$ 368.2118, found 368.2114.

4.3.3.

*(E)-2-(2-(1H-indol-2-yl)vinyl)-1-methyl-4-(4-methylpiperidin-1-yl)quinolin-1-ium iodide (**c3**)*

Brown solid, yield 72%; Melting point: 266–269 °C; ^{1}H NMR (400 MHz, DMSO) δ 11.99 (s, 1H), 8.24 (t, J = 12.9 Hz, 2H), 8.16 (d, J = 6.2 Hz, 2H), 8.09 (d, J = 8.3 Hz, 1H), 7.99 (t, J = 7.9 Hz, 1H), 7.71 (t, J = 7.6 Hz, 1H), 7.57 – 7.51 (m, 1H), 7.49 (s, 1H), 7.40 (d, J = 15.7 Hz, 1H), 7.36 – 7.21 (m, 2H), 4.23 (s, 3H), 4.08 (d, J = 12.8 Hz, 2H), 1.93 (dd, J = 39.1, 10.6 Hz, 2H), 1.83 – 1.69 (m, 1H), 1.50 (dd, J = 22.3, 10.4 Hz, 2H), 1.04 (d, J = 6.4 Hz, 3H). ^{13}C NMR (100 MHz, DMSO) δ 159.8 (s), 153.6 (s), 141.4 (s), 138.9 (s), 135.6 (s), 133.8 (d, J = 56.9 Hz), 133.8 (d, J = 56.9 Hz), 128.4 (s), 127.1 (s), 126.4 (s), 124.9 (s), 121.8 (s), 120.3 (d, J = 27.3 Hz), 119.6 (s), 118.2 – 117.8 (m), 112.0 (s), 109.8 (s), 104.4 (s), 60.8 (s), 52.6 (s), 35.2 (s), 34.1 (s), 19.1 (s). HRMS m/z: calcd. for $C_{26}H_{28}N_3$ $[M - I]^+$ 382.2278, found 382.2275.

*4.3.4. (E)-2-(2-(1H-indol-2-yl)vinyl)-1-methyl-4-(pyrrolidin-1-yl)quinolin-1-ium iodide (**c4**)*

Yellow solid, yield 43%; Melting point: 206 - 213°C; ^{1}H NMR (400 MHz, DMSO) δ 11.77 (s, 1H), 8.51 (d, J = 8.39 Hz, 1H), 8.16 (d, J = 8.8 Hz, 1H), 8.00 (t, J = 7.8 Hz, 1H), 7.88 (d, J = 15.8 Hz, 1H), 7.67 (t, J = 7.7 Hz, 1H), 7.61 (d, J = 8.0 Hz,

1H), 7.55 (d, J = 15.8 Hz, 1H), 7.44 (d, J = 8.19 Hz, 1H), 7.22 (t, J = 7.39 Hz, 1H), 7.05 (t, J = 7.2 Hz, 2H), 6.89 (s, 1H), 4.12 (s, 3H), 4.02 (s, 4H), 2.06 (s, 4H). ^{13}C NMR (100 MHz, DMSO) δ 155.4 (s), 154.7 (s), 152.1 (s), 151.8 (s), 141.3 (s), 138.6 (s), 137.4 (s), 135.6 (s), 133.8 (s), 133.7 (s), 132.9 (s), 132.0 (s), 128.4 (s), 128.2 (s), 127.9 (s), 127.6 (s), 125.5 (s), 125.3 (s), 124.6 (s), 123.8 (s), 121.7 (s), 121.2 (s), 120.6 (s), 120.4 (s), 120.2 (s), 119.0 (s), 118.7 (s), 118.6 (s), 118.2 (s), 111.9 (s), 108.9 (s), 106.5 (s), 103.2 (s), 100.0 (s), 56.5 (s), 53.9 (s), 38.1 (s), 25.7 (s), 19.0 (s). HRMS m/z: calcd. for $C_{24}H_{24}N_3$ $[M - I]^+$ 354.1965, found 354.1958.

*4.3.5. (E)-2-(2-(1H-indol-2-yl)vinyl)-1-methyl-4-morpholinoquinolin-1-iumiodide (**c5**)*

Brown solid, yield 57%; Melting point: 248 - 256°C; ^{1}H NMR (400 MHz, DMSO) δ 11.79 (s, 1H), 8.31 (d, J = 8.9 Hz, 1H), 8.19 (d, J = 7.9 Hz, 1H), 8.06 (dd, J = 14.4, 10.9 Hz, 2H), 7.75 (t, J = 7.59 Hz, 1H), 7.66 (d, J = 3.3 Hz, 1H), 7.63 (d, J = 4.3 Hz, 1H), 7.57 (s, 1H), 7.47 (d, J = 8.19 Hz, 1H), 7.31 (t, J = 7.3 Hz, 1H), 7.07 (t, J = 7.4 Hz, 1H), 7.11 (s, 1H), 4.27 (s, 3H), 3.91 (d, J = 4.4 Hz, 4H), 3.80 (d, J = 4.1 Hz, 4H). ^{13}C NMR (100 MHz, DMSO) δ 159.8 (s), 154.1 (s), 153.8 (s), 141.3 (s), 138.9 (s), 135.5 (s), 134.3 (s), 134.0 (s), 128.4 (s), 127.0 (s), 126.8 (s), 125.1 (s), 121.9 (s), 120.6 (s), 120.2 (s), 119.7 (s), 117.4 (s), 112.0 (s), 110.2 (s), 104.9 (s), 66.3 (s), 52.5 (s), 38.5 (s). HRMS m/z: calcd. for $C_{24}H_{24}N_3O$ $[M - I]^+$ 371.1928, found 371.1924.

*4.3.6. (E)-2-(2-(1H-indol-2-yl)vinyl)-4-((2-(diethylamino)ethyl)amino)-1-methylquinolin-1-ium iodide (**c6**)*

Brown solid, yield 49%; Melting point: 213 - 219°C; ^{1}H NMR (400 MHz, DMSO) δ 11.79 (s, 1H), 8.48 (d, J = 8.3 Hz, 1H), 8.19 (d, J = 9.0 Hz, 1H), 8.03 (t, J = 7.6 Hz, 1H), 7.88 (d, J = 15.8 Hz, 1H), 7.76 (t, J = 7.6 Hz, 1H), 7.61 (dd, J = 16.1, 11.9 Hz, 2H), 7.46 (d, J = 8.19 Hz, 1H), 7.19 (t, J = 7.6 Hz, 1H), 7.08 (s, 1H), 7.06 (t, J = 7.5 Hz, 1H), 6.93 (s, 1H), 4.15 (s, 3H), 3.74 (t, J = 6.3 Hz, 2H), 2.78 (t, J = 6.3 Hz, 2H), 2.58 (dd, J = 14.1, 7.0 Hz, 4H), 0.96 (t, J = 7.0 Hz, 6H). ^{13}C NMR (100 MHz, DMSO) δ 154.2 (s), 154.0 (s), 140.0 (s), 138.7 (s), 135.5 (s), 134.2 (s), 132.5 (s),

128.4 (s), 126.7 (s), 124.7 (s), 123.6 (s), 121.7 (s), 120.4 (s), 119.4 (s), 118.3 (s), 117.8 (s), 111.9 (s), 109.1 (s), 97.0 (s), 51.4 (s), 47.1 (s), 46.9 (s), 42.1 (s), 37.8 (s), 12.3 (s). HRMS m/z: calcd. for $C_{26}H_{31}N_4$ $[M - I]^+$ 399.2543, found 399.2539.

*4.3.7. (E)-2-(2-(1H-indol-2-yl)vinyl)-1-methyl-4-((2-(piperidin-1-yl)ethyl)amino)quinolin-1-ium iodide (**c7**)*

Dark brown solid, yield 65%; Melting point: 190 - 195°C; ^{1}H NMR (400 MHz, DMSO) δ 11.82 (s, 1H), 8.27 (d, J = 8.8 Hz, 1H), 8.11 (d, J = 8.3 Hz, 1H), 8.06 – 7.98 (m, 2H), 7.74 (t, J = 7.59 Hz, 1H), 7.63 (dd, J = 11.8, 9.1 Hz, 2H), 7.48 – 7.39 (m, 2H), 7.19 (t, J = 7.6 Hz, 1H), 7.06 (t, J = 7.5 Hz, 1H), 6.98 (s, 1H), 4.23 (s, 3H), 3.76 (s, 4H), 1.84 (s, 4H), 1.78 (s, 2H). ^{13}C NMR (100 MHz, DMSO) δ 160.0 (s), 153.6 (s), 141.4 (s), 138.9 (s), 135.6 (s), 134.1 (s), 133.5 (s), 129.3 (s), 128.4 (s), 127.0 (s), 126.4 (s), 124.9 (s), 121.8 (s), 120.5 (s), 120.2 (s), 119.6 (s), 117.6 (s), 112.0 (s), 109.8 (s), 104.4 (s), 100.1 (s), 56.5 (s), 53.3 (s), 38.4 (s), 25.9 (s), 24.0 (s), 19.0 (s). HRMS m/z: calcd. for $C_{27}H_{30}N_4$ $[M - I]^+$ 411.2528, found 411.2532.

*4.3.8. (E)-2-(2-(1H-indol-3-yl)vinyl)-1-methylquinolin-1-ium iodide (**c8**)*

Purple solid, yield 78%; Melting point: 253–254 °C; ^{1}H NMR (400 MHz, DMSO-d6) δ 12.31 (s, 1H), 8.81 (d, J = 9.1 Hz, 1H), 8.64 (d, J = 15.5 Hz, 1H), 8.60 (d, J = 9.2 Hz, 1H), 8.44 (d, J = 8.9 Hz, 1H), 8.40 (d, J = 2.8 Hz, 1H), 8.31 – 8.17 (m, 2H), 8.08 (t, J = 7.7 Hz, 1H), 7.84 (t, J = 7.5 Hz, 1H), 7.64 – 7.48 (m, 2H), 7.31 (dd, J = 5.9, 3.0 Hz, 2H), 4.46 (s, 3H). ^{13}C NMR (100 MHz, DMSO) δ 156.1 (s), 156.1 (s), 143.7 (s), 139.6 (d, J = 16.5 Hz), 137.3 (s), 135.5 (s), 135.2 (s), 130.5 (s), 129.2 (s), 128.5 (s), 128.0 (s), 126.0 (s), 122.3 (s), 120.8 (d, J = 5.4 Hz), 119.6 (s), 116.6 (s), 112.6 (s), 112.2 (s). HRMS m/z: calcd. for $C_{20}H_{17}N_2$ $[M - I]^+$ 285.1386, found 285.1383.

*4.3.9. (E)-2-(2-(1H-indol-3-yl)vinyl)-1-methyl-4-(piperidin-1-yl)quinolin-1-ium iodide (**c9**)*

Yellow solid, yield 56%; Melting point: 175 - 185°C; ^{1}H NMR (400 MHz, DMSO) δ 11.99 (s, 1H), 8.24 (dd, J = 16.4, 12.3 Hz, 2H), 8.16 (dd, J = 6.6, 2.6 Hz, 2H), 8.09 (d, J = 8.2 Hz, 1H), 8.00 (t, J = 7.9 Hz, 1H), 7.69 (t, J = 7.6 Hz, 1H), 7.52 (dd, J = 6.3, 2.4 Hz, 1H), 7.50 (s, 1H), 7.41 (d, J = 15.7 Hz, 1H), 7.31 – 7.23 (m, 2H), 4.23 (s, 3H), 3.69 (s, 3H), 1.85 (s, 3H). ^{13}C NMR (100 MHz, DMSO) δ 141.3 (s), 141.2 (s), 137.7 (s), 136.6 (s), 136.6 (s), 133.7 (s), 133.5 (s), 131.7 (s), 131.4 (s), 128.7 (s), 127.7 (s), 127.5 (s), 125.8 (s), 125.5 (s), 125.4 (s), 125.1 (s), 123.2 (s), 122.5 (s), 121.4 (s), 120.6 (s), 120.4 (s), 119.7 (s), 118.7 (s), 118.6 (s), 116.4 (s), 114.1 (s), 113.7 (s), 112.9 (s), 112.6 (s), 110.8 (s), 103.2 (s), 99.4 (s), 53.8 (s), 53.4 (s), 25.7 (s), 25.4 (s). HRMS m/z: calcd. for $C_{25}H_{26}N_3$ $[M - I]^+$ 368.2119, found 368.2124.

4.3.10.

*(E)-2-(2-(1H-indol-3-yl)vinyl)-1-methyl-4-(4-methylpiperidin-1-yl)quinolin-1-ium iodide (**c10**)*

Brown solid, yield 78%; Melting point: 266–269 °C; ^{1}H NMR (400 MHz, DMSO) δ 12.12 (s, 1H), 8.28 – 8.18 (m, 2H), 8.16 (d, J = 2.5 Hz, 2H), 8.07 (d, J = 8.2 Hz, 1H), 7.98 (t, J = 7.8 Hz, 1H), 7.71 (t, J = 7.6 Hz, 1H), 7.57 – 7.50 (m, 1H), 7.48 (s, 1H), 7.39 (d, J = 15.7 Hz, 1H), 7.26 (p, J = 7.7 Hz, 2H), 4.22 (s, 3H), 4.08 (d, J = 12.8 Hz, 2H), 1.87 (d, J = 12.6 Hz, 2H), 1.79 (d, J = 6.1 Hz, 1H), 1.49 (dd, J = 22.0, 10.7 Hz, 2H), 1.03 (d, J = 6.3 Hz, 3H). ^{13}C NMR (100 MHz, DMSO) δ 159.6 (s), 155.5 (s), 141.3 (s), 138.8 (s), 137.8 (s), 133.8 (s), 132.8 (s), 126.9 (s), 126.3 (s), 125.5 (s), 123.4 (s), 121.7 (s), 120.8 (s), 120.4 (s), 119.5 (s), 114.0 – 113.8 (m), 113.2 (s), 113.1 (s), 104.4 (s), 52.5 (s), 38.3 (s), 34.0 (s), 30.5 (s), 22.0 (s). HRMS m/z: calcd. for $C_{26}H_{28}N_3$ $[M - I]^+$382.2278, found 382.2276.

*4.3.11. (E)-2-(2-(1H-indol-3-yl)vinyl)-1-methyl-4-(pyrrolidin-1-yl)quinolin-1-ium iodide (**c11**)*

Brown solid, yield 54%; Melting point: 205 -215°C; ^{1}H NMR (400 MHz, DMSO) δ 12.05 (s, 1H), 8.50 (s, 1H), 8.17 – 8.10 (m, 2H), 8.01 (dt, J = 15.8, 5.3 Hz, 3H), 7.65 (t, J = 7.7 Hz, 1H), 7.51 (d, J = 7.7 Hz, 1H), 7.47 (d, J = 15.7 Hz, 1H), 7.28-7.19 (m,

2H), 7.00 (s, 1H), 4.11 (s, 3H), 4.01 (s, 4H), 2.06 (s, 4H). ^{13}C NMR (100 MHz, DMSO) δ 159.8 (s), 155.6 (s), 141.3 (s), 138.8 (s), 137.8 (s), 133.8 (s), 132.8 (s), 126.8 (s), 126.3 (s), 125.5 (s), 123.4 (s), 121.7 (s), 120.7 (s), 120.4 (s), 119.5 (s), 114.1 (s), 113.3 (s), 113.1 (s), 104.4 (s), 53.2 (s), 38.3 (s), 25.9 (s), 24.0 (s). HRMS m/z: calcd. for $C_{24}H_{24}N_3$ [M - I]$^+$ 354.1949, found 354.1955.

4.3.12. (E)-2-(2-(1H-indol-3-yl)vinyl)-1-methyl-4-morpholinoquinolin-1-ium iodide ***(c12)***

Yellow solid, yield 53%; Melting point: 248 - 255°C; ^{1}H NMR (400 MHz, DMSO) δ 12.03 (s, 1H), 8.30 (dd, J = 12.3, 3.2 Hz, 2H), 8.18 (t, J = 5.2 Hz, 3H), 7.99 (t, J = 7.5 Hz, 1H), 7.73 (t, J = 7.6 Hz, 1H), 7.58 – 7.51 (m, 2H), 7.43 (d, J = 15.7 Hz, 1H), 7.32 – 7.24 (m, 2H), 4.27 (s, 3H), 3.97 – 3.89 (m, 4H), 3.72 (d, J = 4.2 Hz, 4H). ^{13}C NMR (100 MHz, DMSO) δ 159.8 (s), 155.6 (s), 141.3 (s), 138.8 (s), 137.8 (s), 133.8 (s), 132.8 (s), 126.8 (s), 126.3 (s), 125.5 (s), 123.4 (s), 121.7 (s), 120.7 (s), 120.4 (s), 119.5 (s), 114.1 (s), 113.3 (s), 113.1 (s), 104.4 (s), 53.2 (s), 40.6 (s), 40.4 (s), 40.2 (s), 40.0 (s), 39.8 (s), 39.6 (s), 39.4 (s), 38.3 (s), 25.9 (s), 24.1 (s). HRMS m/z: calcd. for $C_{24}H_{24}N_3O$[M - I]$^+$ 371.1928, found 371.1932.

4.3.13.

(E)-2-(2-(1H-indol-3-yl)vinyl)-4-((2-(diethylamino)ethyl)amino)-1-methylquinolin-1-ium iodide ***(c13)***

Yellow-brown solid, yield 49%; Melting point: 213 - 217°C; ^{1}H NMR (400 MHz, DMSO) δ 11.90 (s, 1H), 8.45 (d, J = 8.3 Hz, 1H), 8.18 (d, J = 8.8 Hz, 1H), 8.11 (d, J = 8.19Hz, 1H), 8.06 (d, J = 16.2 Hz, 2H), 8.02 – 7.97 (m, 1H), 7.69 (t, J = 7.59 Hz, 1H), 7.59 (d, J = 6.4 Hz, 1H), 7.38 (d, J = 15.8 Hz, 1H), 7.29 – 7.22 (m, 2H), 7.16 (s, 1H), 4.15 (s, 3H), 3.73 (t, J = 6.4 Hz, 2H), 2.81 (t, J = 6.4 Hz, 2H), 2.61 (q, J = 7.1 Hz, 4H), 1.07 (t, J = 7.1 Hz, 6H). ^{13}C NMR (100 MHz, DMSO) δ 155.7 (s), 153.7 (s), 140.0 (s), 137.8 (s), 137.1 (s), 134.0 (s), 131.7 (s), 126.5 (s), 126.3 (s), 125.5 (s), 123.5 (s), 123.2 (s), 121.4 (s), 120.5 (s), 119.3 (s), 119.0 (s), 117.7 (s), 114.1 (s), 113.8 (s),

113.0 (s), 96.3 (s), 51.4 (s), 47.1 (s), 37.8 (s), 22.8 (s), 12.4 (s). HRMS m/z: calcd. for $C_{26}H_{31}N_4$ $[M - I]^+$ 399.2539, found 399.2534.

4.3.14.

(E)-2-(2-(1H-indol-3-yl)vinyl)-1-methyl-4-((2-(pyrrolidin-1-yl)ethyl)amino)quinolin-1-ium iodide ***(c14)***

Yellow brown solid, yield 74%; Melting point: 205 - 210°C; ^{1}H NMR (400 MHz, DMSO) δ 11.90 (s, 1H), 8.51 (d, J = 8.1 Hz, 1H), 8.21 (d, J = 8.8 Hz, 1H), 8.09 (dd, J = 19.0, 11.8 Hz, 3H), 8.02 – 7.97 (m, 1H), 7.73 (t, J = 7.6 Hz, 1H), 7.53 (d, J = 7.1 Hz, 1H), 7.38 (d, J = 15.8 Hz, 1H), 7.29 – 7.19 (m, 2H), 7.14 (s, 1H), 4.15 (s, 3H), 3.79 (t, J = 6.3 Hz, 2H), 2.86 (s, 2H), 2.61 (s, 4H), 1.71 (s, 4H). ^{13}C NMR (100 MHz, DMSO) δ 155.8 (s), 153.7 (s), 140.0 (s), 137.8 (s), 137.3 (s), 134.0 (s), 131.8 (s), 126.3 (s), 125.5 (s), 123.9 (s), 123.2 (s), 121.4 (s), 120.5 (s), 119.2 (s), 117.8 (s), 114.0 (s), 113.8 (s), 113.0 (s), 96.3 (s), 79.8 (s), 79.5 (s), 79.1 (s), 66.7 (s), 56.8 (s), 53.9 (s), 37.8 (s). HRMS m/z: calcd. for $C_{26}H_{29}N_4$ $[M - I]^+$ 397.2381, found 397.2376.

4.3.15.

(E)-2-(2-(1H-indol-3-yl)vinyl)-1-methyl-4-(3-morpholinopropyl)quinolin-1-ium iodide ***(c15)***

Yellow brown solid, yield 45%; Melting point: 145 - 149°C; ^{1}H NMR (400 MHz, DMSO) δ 11.97 (s, 1H), 8.89 (s, 1H), 8.57 (d, J = 8.03 Hz, 1H), 8.20 (d, J = 8.79 Hz, 1H), 8.20 – 8.02 (m, 3H), 8.01 – 7.85 (m, 1H), 7.72 (t, J = 7.6 Hz, 1H), 7.49 (d, J = 8.2 Hz, 1H), 7.4 (d, J = 15.8 Hz, 1H), 7.25 (t, J = 5.6 Hz, 2H), 7.16 (s, 1H), 4.15 (s, 3H), 3.80 (d, J = 4.8 Hz, 2H), 3.58 (s, 4H), 2.73 (s, 2H), 2.53 (d, J = 8.9 Hz, 4H). ^{13}C NMR (100 MHz, DMSO) δ 155.8 (s), 153.7 (s), 140.0 (s), 137.8 (s), 137.3 (s), 134.0 (s), 131.8 (s), 126.3 (s), 125.5 (s), 123.9 (s), 123.2 (s), 121.4 (s), 120.5 (s), 119.2 (s), 117.8 (s), 114.0 (s), 113.8 (s), 113.0 (s), 96.3 (s), 79.8 (s), 79.5 (s), 79.1 (s), 66.7 (s), 56.8 (s), 53.9 (s), 37.8 (s). HRMS m/z: calcd. for $C_{27}H_{30}N_3O$[M - I]$^+$ 413.2329, found 413.2331.

4.4. Antibacterial susceptibility assays

The minimum inhibitory concentrations (MICs) of the test compounds were determined using the broth micro-dilution procedure described in the Clinical and Laboratory Standards Institute (CLSI) guidelines.[19] Two or three single colonies of the testing bacterial strain on a TSB agar plate were inoculated in 5 mL of MH or CA-MH broth and then grown at 37 ºC overnight with shaking. The bacterial culture was transferred to fresh MH or CA-MH broth and diluted to a final concentration of approximately 5× 10^5 CFU/mL in a 96-well microtiter plate. Then, a series of concentrations of the test compounds were added. After 18 h of incubation at 37 ºC, The MIC value is defined as the lowest concentration of test compounds which prevents visible growth of bacterium.

4.5. Minimum bactericidal concentration (MBC) assay

MBC assay was conducted using the broth microdilution assay described in the above section. The MBC was determined by plating 10 μL of culture volume from the MIC assay onto TSB agar plate and colony formation was examined after 24 hours at 37°C. MBC is defined as the lowest compound concentration resulting in a $\geqq$ 3-log reduction in the number of colony forming units (CFU) [24].

4.6. Time-killing kinetics assay

A growing culture of *S. aureus* ATCC BAA41 was diluted to approximately 10^6 CFU. mL^{-1} in volumes of Mueller Hinton broth. The bacterial culture was grown in the presence of various concentrations (0×, 1×, 2×, 4×MIC) of compounds and incubated at 37 ºC with shaking. At the appropriate time intervals (0, 1, 2, 4, 8, 24h), 100 μL of culture were removed for serial dilutions in appropriate times, and 30 μL was spread on MH agar plates. The cell counts ($CFU.mL^{-1}$) were recorded after incubating the plates at 37 ºC for 24 h.

4.7. Drug resistance study

The drug resistance study was based on the minimum inhibitory concentrations (MICs) tests. The initial MIC values of two compounds and two control antibiotics (rifampin and norfloxacin) against *S. aureus* ATCC 29213 were determined as described above. The bacterial culture from 96-well microtiter plate at a concentration of 0.5× MIC was continuously used to prepare the bacterial dilution (approximately 5×10^5 CFU/mL) for the next MIC assay. Then these bacterial suspensions were seeded into another new 96-well microtiter plate and incubated with various concentrations of two compounds and the two control antibiotics. After incubation for 24 h at 37 °C, the fold change of MIC values was determined. This process was repeated for about 17 passages.

4.8. Visualization of bacterial morphology and membrane staining

The *B. subtilis* 168, stored at -80 ºC, was transferred into LB medium and grown at 37ºC with shaking overnight. The cultures were then diluted to approximately 1×10^5 CFU/mL and inoculated in the same medium containing absence or MIC concentration of the test compounds. After grown at 37 ºC for 4 h, the cells for bacterial morphology were harvested by centrifugation and then resuspended in 100 microliter phosphate buffered saline buffer (PBS, pH 7.4). For membrane staining, the cells were stained by a red fluorescent dye FM4-64 (1.6 μM, Invitrogen, Eugene, OR, USA) for 15 min at 37 °C without shaking. Then the procedure of cell harvest was performed as previously described. Five microliter of sample mixtures were placed on a microscopic slide pretreated with 0.1% (w/v) poly-L-lysine. The bacterial cell morphology was visualized using microscopy with a 40× magnification. The membrane staining of cells was observed using fluorescence microscopy with a 40× magnification. The images were captured using a super high-resolution laser confocal microscopy (Carl Zeiss, LSM 800 with Airyscan). The scale bar is 20 μm. Each assay was performed in triplicates.

4.9. GTPase activity assay

GTPase Activity of *Sa*FtsZ was determined in 96- well micro plates using the ATPase/GTPase Activity Assay Kit (SIGMA-ALDRICH, MAK113) according to an optimized protocol and the manufacturer's instructions.[25] In this assay, 10 μL *Sa*FtsZ (4.6 μM) protein was pre-incubated with 10 μL vehicle (1% DMSO) or serial dilutions of the test compounds in assay buffer (40 mM Tris, 80 mM NaCl, 8 mM $MgAc_2$, 1 mM EDTA, pH 7.5, containing 0.01% Triton X-100 to avoid compound aggregation) for 10 min at room temperature. Then 30μL GTP (0.4 mM) was added into the reaction mix and incubated at 37ºC about 30 min. Then 50 μL of reactions system were quenched by adding 200 μL of reagent for 30 min at 37ºC to terminate the enzyme reaction. The concentration of inorganic phosphate was measured by reading the absorbance at 620 nm with a microplate reader.

4.10. Light scattering assay

The overexpression and purification of *S. aureus* FtsZ were carried out according to the method as described in this literature.[26] Light scattering assay was performed following the procedure as described in this work.[27] Briefly, the polymerization and depolymerization of recombinant *S. aureus* FtsZ was measured by using a thermostatically (37 ºC) fluorescence spectrometer (Perkin Elmer, USA) in a model of 90° light scattering. Both excitation and emission wavelengths were set to 600 nm with a slit width of 2.5 nm. *S. aureus* FtsZ (12 μM) in 50 mM of MOPS buffer (pH 6.5) was incubated with vehicle (1% DMSO) or different concentrations of the test compounds. 50 mM KCl and 10 mM $MgCl_2$ were then added to establish a baseline. A final concentration of 1 mM GTP was added after that. The variation in light scattering was measured for an additional 2000s. All experimental data have been subtracted appropriate blanks. Each assay was performed in triplicate.

4.11. Antibacterial activity against FtsZ over-expression strain.

588 The strain was constructed following previous study.[28] The FtsZ was over
589 expressed by incubating with 0.4 mM IPTG. The general procedure of antibacterial
590 activity assay was mentioned in section 4.4.
591
592 *4.12. Molecular docking study*
593 The molecular modeling procedures were performed using Discovery Studio
594 2016. The X-ray crystal structure of *Sa*FtsZ downloaded from the PDB database
595 (PDB entry: 4DXD; resolution: 2.0 Å).[29] Water molecules and co-crystal ligands were
596 removed from the structure and the protein was prepared for docking using an
597 automated procedure of Discovery Studio (DS). The ligand **c2** were sketched and
598 prepared for docking using the tools of small molecules of DS. Automated docking
599 studies were carried out using DS-CDocker protocol of DS. The top-scoring poses
600 were visually inspected.

601 **Acknowledgements**

602 We acknowledge the support from the National Natural Science
603 Foundation of China (81703333 and 81473082), Natural Science Foundation of
604 Guangdong Province, China (2017A030313078), and Science and Technology
605 Program of Guangdong Province (2016A020209009, 2016B020211002 and
606 510093637143), and Department of Agriculture and Rural Affairs of
607 Guangdong Province, China (2018LM2175). The authors are also grateful to
608 the support from Nanshan Scholar Program of Guangzhou Medical University
609 (B185006006008) and Innovation and Technology Commission of Hong Kong,
610 The Hong Kong Polytechnic University.
611

612 **Notes and References**

613 1. Willyard C. The drug-resistant bacteria that pose the greatest health threats.
614 *Nature.* 2017;543(7643):15.
615 2. Kim W, Zhu W, Hendricks GL, et al. A new class of synthetic retinoid
616 antibiotics effective against bacterial persisters. *Nature.* 2018;556(7699):103-107.
617 3. Wright GD. Antibiotics: a new hope. *Chem Biol.* 2012;19(1):3-10.

4. Sass P, Brotz-Oesterhelt H. Bacterial cell division as a target for new antibiotics. *Curr Opin Microbiol.* 2013;16(5):522-530.

5. Hurley KA, Santos TM, Nepomuceno GM, Huynh V, Shaw JT, Weibel DB. Targeting the Bacterial Division Protein FtsZ. *J Med Chem.* 2016;59(15):6975-6998.

6. Yang X, Lyu Z, Miguel A, McQuillen R, Huang KC, Xiao J. GTPase activity-coupled treadmilling of the bacterial tubulin FtsZ organizes septal cell wall synthesis. *Science.* 2017;355(6326):744-747.

7. Du S, Pichoff S, Lutkenhaus J. FtsEX acts on FtsA to regulate divisome assembly and activity. *Proc Natl Acad Sci U S A.* 2016;113(34):E5052-5061.

8. Haranahalli K, Tong S, Ojima I. Recent advances in the discovery and development of antibacterial agents targeting the cell-division protein FtsZ. *Bioorg Med Chem.* 2016;24(24):6354-6369.

9. Ma S, Ma S. The Development of FtsZ Inhibitors as Potential Antibacterial Agents. *ChemMedChem.* 2012;7(7):1161-1172.

10. Margalit DN, Romberg L, Mets RB, et al. Targeting cell division: small-molecule inhibitors of FtsZ GTPase perturb cytokinetic ring assembly and induce bacterial lethality. *Proc Natl Acad Sci U S A.* 2004;101(32):11821-11826.

11. Sun N, Du RL, Zheng YY, et al. Antibacterial activity of N-methylbenzofuro[3,2-b]quinoline and N-methylbenzoindolo[3,2-b]-quinoline derivatives and study of their mode of action. *Eur J Med Chem.* 2017;135:1-11.

12. Mathew B, Ross L, Reynolds RC. A novel quinoline derivative that inhibits mycobacterial FtsZ. *Tuberculosis.* 2013;93(4):398-400.

13. Sun N, Lu YJ, Chan FY, et al. A Thiazole Orange Derivative Targeting the Bacterial Protein FtsZ Shows Potent Antibacterial Activity. *Front Microbiol.* 2017;8:855.

14. Bi F, Guo L, Wang Y, et al. Design, synthesis and biological activity evaluation of novel 2,6-difluorobenzamide derivatives through FtsZ inhibition. *Bioorg Med Chem Lett.* 2017;27(4):958-962.

15. Kolb HC, Finn MG, Sharpless KB. Click Chemistry: Diverse Chemical Function from a Few Good Reactions. *Angew Chem Int Ed Engl.* 2001;40(11):2004-2021.

16. Lu YJ, Guo XL, Xu MH, et al. Selective visualization of DNA G-quadruplex structures in live cells with 1-methylquinolinium-based molecular probes: The importance of indolyl moiety position towards specificity. *Dyes and Pigments.* 2017;143:331-341.

17. Wang C, Lu YJ, Cai SY, et al. Advancing small ligands targeting RNA for better binding affinity and specificity: A study of structural influence through molecular design approach. *Sensor Actuat B-Chem.* 2018;262:386-394.

18. Xia CL, Wang N, Guo QL, et al. Design, synthesis and evaluation of 2-arylethenyl-N-methylquinolinium derivatives as effective multifunctional agents for Alzheimer's disease treatment. *Eur J Med Chem.* 2017;130:139-153.

19. Wikler MA, Hindler JF, Cookerill FR, Patel JB, Bush K, Powell M. Methods for Dilution Antimicrobial Sucseptibility Tests for Bacteria That Grow Aerobically. 2009;29:M07-A08.

20. Bi FC, Song D, Zhang N, et al. Design, synthesis and structure-based optimization of novel isoxazole-containing benzamide derivatives as FtsZ modulators. *Eur J Med Chem.* 2018;159:90-103.

21. Sun N, Du RL, Zheng YY, et al. Antibacterial activity of 3-methylbenzo[d]thiazol-methylquinolinium derivatives and study of their action mechanism. *J Enzyme Inhib Med Chem.* 2018;33(1):879-889.

22. Bisson-Filho AW, Hsu YP, Squyres GR, et al. Treadmilling by FtsZ filaments drives peptidoglycan synthesis and bacterial cell division. *Science.* 2017;355(6326):739-743.

23. Lu Y-J, Guo X-L, Xu M-H, et al. Selective visualization of DNA G-quadruplex structures in live cells with 1-methylquinolinium-based molecular probes: The importance of indolyl moiety position towards specificity. *Dyes and Pigments.* 2017;143:331-341.

24. Dias FRF, Novais JS, Devillart TADS, et al. Synthesis and antimicrobial evaluation of amino sugar-based naphthoquinones and isoquinoline-5,8-diones and their halogenated compounds. *Eur J Med Chem.* 2018;156:1-12.

25. Zheng YY, Du RL, Cai SY, et al. Study of Benzofuroquinolinium Derivatives as a New Class of Potent Antibacterial Agent and the Mode of Inhibition Targeting FtsZ. *Front Microbiol.* 2018;9.

26. Sun N, Zheng YY, Du RL, et al. New application of tiplaxtinin as an effective FtsZ-targeting chemotype for an antimicrobial study. *Medchemcomm.* 2017;8(10):1909-1913.

27. Chan KF, Sun N, Yan SC, et al. Efficient Synthesis of Amine-Linked 2,4,6-Trisubstituted Pyrimidines as a New Class of Bacterial FtsZ Inhibitors. *ACS Omega.* 2017;2(10):7281-7292.

28. Chan FY, Sun N, Neves MAC, et al. Identification of a New Class of FtsZ Inhibitors by Structure-Based Design and in Vitro Screening. *J Chem Inf Model.* 2013;53(8):2131-2140.

29. Tan CM, Therien AG, Lu J, et al. Restoring Methicillin-Resistant Staphylococcus aureus Susceptibility to beta-Lactam Antibiotics. *Sci Transl Med.* 2012;4(126):126ra135.